THE JOURNAL OF PHYSICAL CHEMISTRY B

Article

pubs.acs.org/JPCB

Atomistic Simulations of Dilute Polyelectrolyte Solutions

Soohyung Park, Xiao Zhu, and Arun Yethiraj*

Department of Chemistry, University of Wisconsin, Madison, Wisconsin, 53706 United States

ABSTRACT: The properties of short chains of poly-(styrene)-*co*-(styrene sulfonate) are studied using atomistic molecular dynamics simulations with explicit solvent. We study single 8-mers and 16-mers with two species of counterions, Na^+ and Mg^{2+}, and for various degrees of sulfonation, *f*. We find that single trajectories do not efficiently sample configurational space, even for fairly long 100-ns simulations, because of rotational barriers caused by nonbonded interactions. Hamiltonian replica exchange molecular dynamics (HREMD) simulations or averages over multiple trajectories are required in order to obtain equilibrium properties. A polystyrene sulfonate chain adopts collapsed conformations at low *f*, in which the sulfonate groups are located outside the globule and benzene rings form the inner region, and adopts extended conformations as *f* is increased. Interestingly, the pair correlation functions between side groups of polystyrene chains are not sensitive to *f* and species of counterion, i.e., the balance of electrostatic repulsion between charged groups and hydrophobic attraction between benzene rings is achieved by conformational change in a way preserving pair correlations between side groups in a polymer chain. For Na^+ counterions, no localization is observed in the simulations. For Mg^{2+} counterions, there is a large free energy barrier to contact pair formation between the sulfonate groups and the Mg^{2+} counterions. As a consequence we do not observe the formation or breaking of contact pairs during the course of a simulation. The simulations provide insight into the important interactions and correlations in polyelectrolyte solutions.

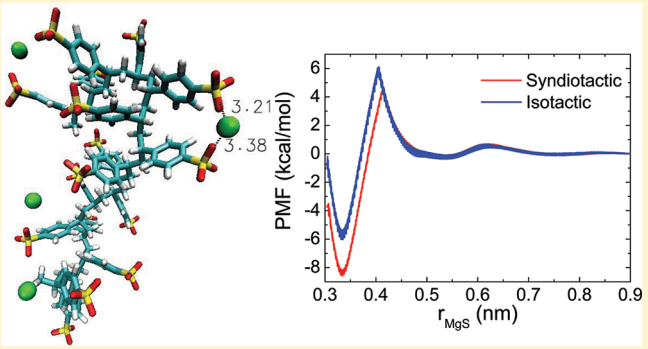

I. INTRODUCTION

Polyelectrolyte solutions are of fundamental interest because of the fascinating range of properties they can display and of practical interest because of the large number of applications. Although they have been actively studied for a number of decades,[1−6] there continue to be many important open questions. Interestingly, the majority of theoretical work has focused on universal properties, and the models used in computer simulation studies have been quite simple. In this paper we present atomistic simulations of short chains of polystyrene sulfonate in water.

The physical properties of polyelectrolytes are the result of a balance between the hydrophobic interactions of the backbone and electrostatic interactions of the polar side groups. Perhaps the most widely studied experimental system is sodium polystyrene sulfonate (NaPSS) in water, and in this case the solvent quality is poor for the polymer backbone and the sulfonated groups are necessary for the polymer to dissolve in water. The competition between the electrostatic repulsions and the solvent-induced attractive interactions in polyelectrolyte solutions results in interesting static and dynamic properties.

Much of our understanding of the static behavior of synthetic polyelectrolyte solutions comes from scattering (light, neutron, and X-ray) experiments.[7−16] For solutions with low ionic strength, scattering experiments are in accord with the predictions of scaling theory,[17] the double-screening theory,[18] and integral equation theories,[19−24] except at low wave-vectors. For high ionic strength and in the presence of multivalent counterions the conformational behavior is more complex and not well understood.

The majority of computational work on polyelectrolytes has focused on generic models, such as freely jointed chains where each bead contains a charge.[21,22,25−32] These models are a good starting point and are expected to be adequate for universal properties. They are not intended, however, to address more detailed questions. One can argue that polyelectrolyte solutions are a particular case where details might matter. In PSS experiments, the degree of polymerization, *N*, is typically between 40 and 700.[7] In this work we find that a single statistical "bead" is at least 16 monomers, which implies that most experimental systems are not in the asymptotic infinite *N* limit.

There are many reasons to believe generic models might not be adequate. Previous work has shown that the solvent plays an important role even in primitive models of polyelectrolyte solutions.[33−35] A simple implicit solvent model, where the solvent is replaced by an effective pairwise attraction between the polymer beads, is inadequate. For a number of different properties this model for the solvent can result in qualitatively

Received: August 23, 2011
Revised: March 19, 2012
Published: March 20, 2012

Table 1. Configuration and Sulfonation of PSS Chains

			configuration[a]															
	$N = 8$				S		R		S		S		R		S		R		R	
f	0.75				s[b]				s		s		s				s		s	
	0.5		1				s		s				s				s			
			2		s								s		s		s			
			3		s				s								s		s	
	0.25				s										s					
$N = 16$			S	R	S	S	R	S	R	R	S	S	R	R	S	R	R	S		
f	0.75		s		s	s	s	s		s	s	s		s	s		s	s		
	0.5	1		s	s		s		s		s				s	s	s			
		2	s				s	s	s		s		s			s	s			
		3	s		s			s	s			s	s		s		s			
	0.25		s					s			s		s							

[a]Configuration of monomeric unit: R (rectus), S (sinister). [b]s: sulfonated side group.

different predictions for the polymer properties compared to a model where the solvent molecules are incorporated explicitly. For the collapse dynamics of a neutral homopolymer the explicit solvent model showed a rapid collapse under all conditions whereas in the implicit solvent model the polymer was trapped in local minima.[36] For polyelectrolyte solutions, explicit solvent simulations showed phase separation[37] while implicit simulations suggested the formation of gel-like structures. Dramatic differences are also seen for the conformational properties of single chains in the bulk and at surfaces.[33−35]

Another possibly important feature of polyelectrolytes is that the local geometry restricts the placement of the charged moieties relative to the backbone. There is therefore local heterogeneity in the electric field and nonelectrostatic interactions near the polymer molecule. Given the subtle nature of the balance between the electro-static and nonpolar interactions, short-ranged dispersion interactions could play an important role in the solution properties.

There have been some recent simulations of atomistic models of synthetic polyelectrolytes.[38−43] Molnar and Rieger[40] reported simulations of an isolated 20-mer sodium poly(acrylic acid) polymer chain (with all monomers deprotonated) in explicit water with Ca^{2+} counterions. They showed a Ca^{2+} ion first bound to the acrylate monomer thus distorting the Na^+ distribution. Different shielded monomers were then attracted to each other. Their simulations used only one initial configuration and were run for 2 ns. Chialvo and Simonson[41] reported atomistic simulations of 10 8-mer PSS chains in water with Li^+ counterions, and added $BaCl_2$ and $LaCl_3$ salt, and investigated the effect of degree of sulfonation and distribution along the chain on the conformational properties and solvation structure. They did not observe any compact structures or compaction by multivalent counterions. These simulations were also fairly short (4 ns). More recently, Carrillo and Dobrynin[43] reported 50 ns simulations of NaPSS with explicit and implicit solvent, for degrees of polymerization ranging from 8 to 64, and for various degrees of sulfonation. For low degrees of sulfonation the chains were compact but became extended when the degree of sulfonation was increased. They showed that, although the compact conformations were similar with implicit and explicit solvent, the extended conformations showed large differences, although they did not report explicit solvent simulations for $N > 16$ when the conformations were extended. They did not study the effect of divalent counterions.

In this work, we perform atomistic molecular dynamics (MD) simulations of a solution of short polystyrene sulfonate (PSS) in water and study the dependence of properties of PSS on the degree of sulfonation, distributions of sulfonated groups along the backbone, and valence of counterions. We find that single MD trajectories of PSS chains do not efficiently sample conformational space in the intended ensemble because of large barriers to torsional rotations. This raises questions about the accuracy of previous simulations. We show that Hamiltonian replica exchange molecular dynamics (HREMD) simulations sample space more effectively than MD simulations. One can also obtain adequate sampling by averaging over multiple independent MD simulations.

We find that PSS chains are collapsed for low degrees of sulfonation with the aromatic rings in the interior and the sulfonate groups on the exterior, as has been noted previously.[43] For partially sulfonated polymers the conformational properties (but not pair correlation functions) are sensitive to the location of the sulfonate groups.

The Na^+ counterions are strongly correlated with the sulfonate groups, but we see no evidence for counterion condensation or localization. There is a large free energy barrier for the formation of a Mg^{2+} contact pair with the sulfonate group, because the Mg^{2+} ions have a very strong hydration shell. As a consequence we do not observe contact pair formation in simulations, and if any contact pairs are initially present they persist through the entire simulation. Even the HREMD simulations are not sufficient to study PSS solutions with Mg^{2+} counterions.

Interestingly, compared to Mg^{2+} counterions, the Na^+ counterions are more strongly correlated with the sulfonate groups, because the Mg^{2+} counterions are more strongly hydrated. We see no evidence for counterion condensation or localization for the initial configurations in which counterions were randomly placed.

The rest of paper is organized as follows. Simulation details are presented in section II, results and presented and discussed in section III, and some conclusions are presented in section IV.

II. SIMULATION DETAILS

Molecular dynamics (MD) simulations are performed for degrees of polymerization N of 8 and 16 and for sulfonation fractions (f) of 0.25, 0.5, 0.75, and 1. For PSS chains with $f = 0.5$, simulations are performed for three different choices of sulfonated groups. The configuration of PSS chains and the

dx.doi.org/10.1021/jp208138t | J. Phys. Chem. B 2012, 116, 4319−4327

position of sulfonated side groups are given in Table 1. The solvent (water) is treated explicitly using the TIP3P water model. Both ends of the PSS chains are terminated with CH_3 groups. All simulations were performed with a modified version of GROMACS 4.0.5.[44] We use the CHARMM22[45] forcefield for all sites except the water molecules, with modifications made for implementation in GROMACS. The CHARMM forcefield parameters for benzene sulfonate groups are taken from existing forcefield parameters for other groups based on similarity. The nonbonded and angle potentials are implemented in a straightforward fashion. The dihedral potential terms are converted into a Ryckaert-Bellmann (RB) potential. More details regarding the implementation can be found in ref 46. The implemented forcefield parameters are tested by comparing the single-point potential energy of PSS molecules to those obtained in the CHARMM package. The simulation cell is a rectangular parallelepiped with periodic boundary conditions in all directions. A cut off distance 1.4 nm is used for nonbonded neighbor list and van der Waals interactions. The particle mesh Ewald method is used for Coulomb interactions. The integration time step is 2 fs for all the simulations, with bond lengths constrained with the LINCS algorithm.

Initial configurations of the PSS chain with counterions and water molecules are prepared as follows. For each N and f, a rectangular simulation box which contains an extended conformation of a PSS chain, counterions, and water molecules is prepared (the minimum distance between the PSS chain and the wall of the simulation box is set to be 1.4 nm) and the energy is minimized using the steepest descent method. This configuration is then simulated for 1.5 ns under isothermal−isobaric (NPT) conditions at p = 1 bar and T = 450 K, using the Nosè-Hoover thermostat (coupling time 0.5 ps) and the Parrinello-Rahman barostat (coupling time 1.0 ps). Three initial configurations are then taken from configurations at t = 0.5, 1.0, and 1.5 ns from this simulation.

Care is taken to ensure that there are no contact pairs between the sulfonate group and the Mg^{2+} counterions in the initial configuration. This is done because contact ion pairs between Mg^{2+} counterions and sulfonate groups are long-lived and persist throughout the course of the simulation. The simulations with Mg^{2+} counterions therefore sample a well-defined subset of the intended ensemble although this might not be representative of the experimental situation.

For each of the three initial configurations generated above, two sets of simulations were performed: A 100-ns MD simulation and a 16-ns Hamiltonian replica exchange MD (HREMD) simulation with eight replicas (details are given in the Appendix). In both cases simulations are at constant NPT with p = 1 bar and at T = 300 K. For HREMD simulations, the strength of Lennard-Jones (LJ) interactions between PSS atoms and the charges of PSS atoms are scaled for each replica to achieve the average probability of replica exchange between neighboring replicas of approximately 0.2 −0.3. We use in-house python wrapper to control HREMD, which is not supported by GROMACS. For all MD/HREMD simulations trajectories and energies are saved in every 1000 steps (2 ps) and the first 25/4-ns of simulations are excluded from the analysis.

III. RESULTS AND DISCUSSION

A. Comparison between MD with HREMD Simulations. We find that the chain does not sample configurational space over the course of a single MD simulation. Figure 1 shows the average (over independent MD trajectories) number of transitions between trans and gauche states of the dihedral angles of the backbone. Except the terminal dihedral angles, the rotation of dihedral angles occurs only a few times during the course of a 100 ns simulation. The average lifetime, τ, of the states are roughly 3.75 and 15 ns for terminal and inner dihedral angles, respectively. We estimate a rotational barrier, $\Delta G^{\ddagger}$, of $8k_BT$ and $10k_BT$, respectively, for terminal and inner dihedral angles, from $\tau = \tau_0 \exp[\Delta G^{\ddagger}/(k_BT)]$, where τ_0 = 1 ps and k_B is Boltzmann's constant.

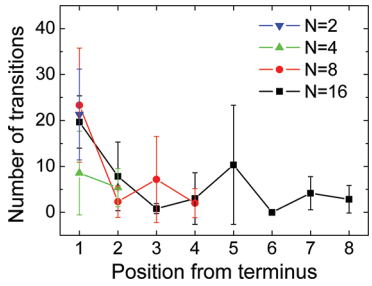

Figure 1. Average number of transitions between trans and gauche states of the dihedral angles of the backbone PSS with Na^+ counterions for f = 1, over a period of 100 ns. The position from the terminus increases as one goes toward the middle of the chain. Except for the terminal dihedral angle (position from terminus equals 1) the number of transitions is very small. Averages are over independent MD trajectories and error bars are one standard deviation about the mean.

As a result, the sampling of conformations is restricted, in which only one of either gauche-(+) or gauche-(-) states is observed in addition to trans state, depending on the streosequence of diad of the segment of PSS chains. As a consequence, the distributions of radius of gyration (r_g) for the backbone of PSS chains shows trajectory to trajectory variation, as shown in Figure 2. We infer that the conformational properties of even such short chains cannot be sampled in a single MD trajectory. We also conclude that it will not be possible to sample efficiently from a single simulation even if

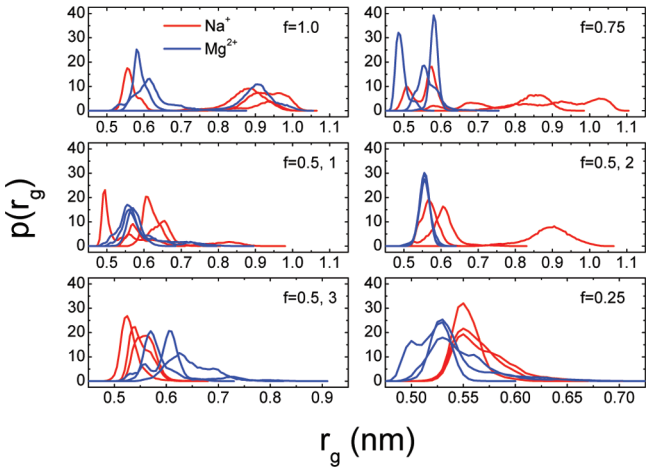

Figure 2. Molecular dynamics simulation results for the distribution of radius of gyration for N = 16 and various values of f. Each curve is the result obtained with a different initial configuration, with distributions with Na^+ counterions in red and those for Mg^{2+} counterions in blue. The three different graphs for f = 0.5 correspond to different placements of the sulfonate group. Note the trajectory to trajectory variation in the distribution function in almost all cases.

dx.doi.org/10.1021/jp208138t | J. Phys. Chem. B 2012, 116, 4319−4327

very long trajectories were used since very few dihedral angle transitions are observed. Furthermore, since the sampling problem is independent of the charge state of the polymer, we deduce that nonelectrostatic (steric) interactions are responsible.

The statistical average over MD simulations performed with the three different initial configurations, however, agrees with results from the HREMD simulations. Figure 3 compares the

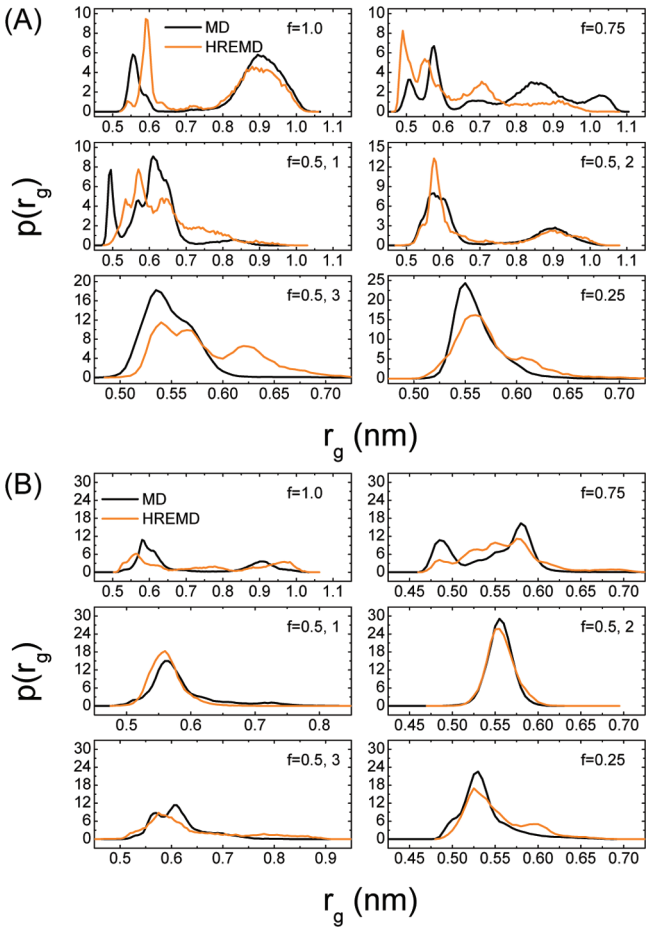

Figure 3. Comparison of HREMD simulations to MD simulations (averaged over the three initial configurations) for the distribution of the radius of gyration, with (A) Na^+ and (B) Mg^{2+} counterions.

distribution of r_g obtained from HREMD simulations to that obtained by averaging over the three MD simulations. There are a sufficiently large number of exchanges in the HREMD simulations that these results are reliable. The disadvantage is that HREMD simulations are very computationally intensive, and cannot be used to study dynamic properties. In general, reasonably good agreement is found between the two types of simulations. Even in the worst case, the positions of the peak in the distributions are in agreement. The agreement in intrachain and counterion-sulfonate group radial distribution functions is even better between two methods (essentially indistinguishable). One can therefore perform simulations either with HREMD or by averaging over many independent MD trajectories, provided the initial configurations correspond to different basins in the free energy landscape. Note that the agreement between HREMD and MD simulations can be improved by considering a larger number of initial configurations in conventional MD.

B. Chain Conformations. The balance of electrostatic repulsion between the charged groups and hydrophobic attraction between benzene rings is reflected in the conformations, which varies from collapsed to extended as f increases from 0 to 1. As is expected the chain adopts conformations where the hydrophobic moieties (including benzene rings) are buried and the charged groups are exposed to the solvent. Representative conformations of $N = 16$ chains (with Na^+ counterions) are shown in Figure 4. For $f = 0.25$ the

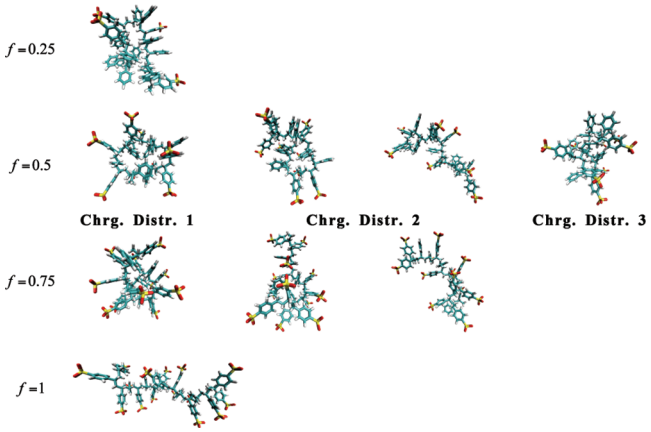

Figure 4. Snapshots of typical conformations of $N = 16$ chains with Na^+ counterions. The oxygen atoms are shown in red, sulfur atoms in yellow, hydrogen atoms in white, and carbon atoms in cyan.

chain is collapsed and for $f = 1$ the chain is fully expanded. The other two values of f correspond to intermediate chain conformations. An arrangement of side groups so that the unsulfonated styrene groups are buried and the sulfonated groups are exposed is also observed for $f = 0.5$ and 0.75. For $f = 0.5$ the chain conformations are sensitive to the sequence of sulfonated groups. Different chemical isomers (which correspond to different placements of the sulfonate groups) have very different conformations, with the chain collapsed in cases 1 and 3 and partially expanded in case 2.

An important point to note is that the collapse of these oligomers occurs through the rotation of only one dihedral angle. Although the collapsed conformations appear to be quite globular they consist of two relatively stretched segments folded over each other. This manner of collapse is very different from what is seen in generic models, where the backbone atoms collapse into a spherical globule.

For PSS chains with Mg^{2+} counterions, in some cases the chains adopt more compact conformations than those with Na^+ counterions (for the same value of f and N) but in other cases they are more expanded (see Figure 2). In fact, for some sequences with $f = 0.5$ there is a bimodal distribution in $p(r_g)$ with Na^+ counterions but not with Mg^{2+} counterions. These differences are probably due to a balance between the correlation between counterions and sulfonate groups (stronger for Na^+ counterions) and the entropy of the counterions, and we do not have a simple physical explanation. The general trends, namely, burial of hydrophobic groups, exposure of charged groups, and sequence dependence of the conformations is observed with Na^+ and Mg^{2+} counterions.

The mean square radius of gyration $\langle r_g^2 \rangle$, depicted in Figure 5. Differently from conformations and $p(r_g)$, $\langle r_g^2 \rangle$ is independent of f except for $N = 16$ with Na^+ counterions.

dx.doi.org/10.1021/jp208138t | J. Phys. Chem. B 2012, 116, 4319–4327

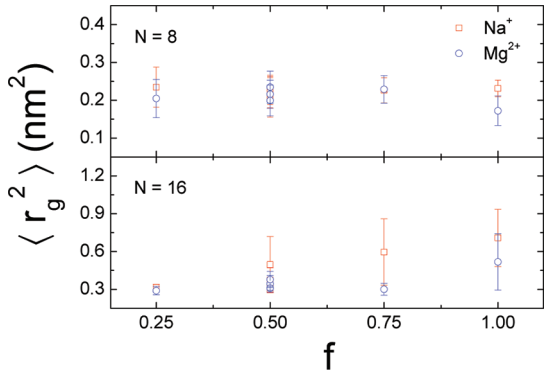

Figure 5. Mean square radius of gyration as a function of degree of sulonation f. The error bars are one standard deviation about the mean.

This may indicate that a single statistical bead is at least 16 monomers.

C. Intrachain Pair Correlation Functions. The correlation between sulfur atoms is consistent with these groups being spread out on the exterior of the globule. Figure 6 depicts the

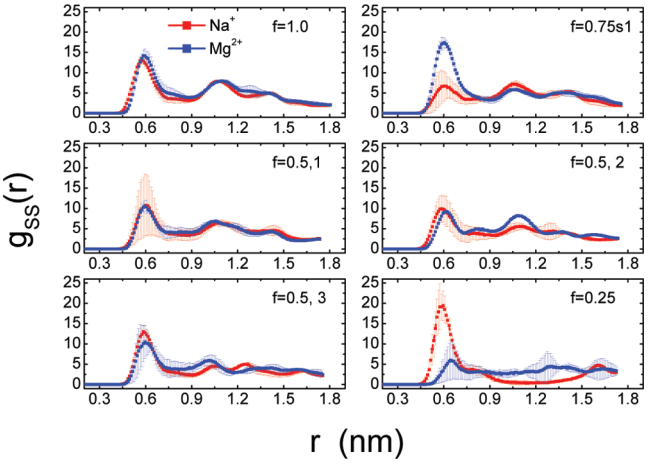

Figure 6. Pair correlation function between sulfur atoms, $g_{SS}(r)$, for N = 16 and various values of f with Na^+ (red curves) and Mg^{2+} (blue curves) counterions. For f = 0.5 the different graphs correspond to different sequence isomers. The error bars are one standard deviation about the mean.

pair correlation function between sulfur atoms in the SO_3^- groups, $g_{SS}(r)$, for N = 16. For f = 1 there are three characteristic peaks: At r = 0.6 nm, which corresponds to the distance between the closest charged groups along the backbone, and r = 1.1 nm and r = 1.4 nm, which represent the correlation between distant SO_3^- groups. For the other values of f the peaks in $g_{SS}(r)$ occur at the same positions, but the intensities depend on f and the type of counterion. For f = 0.5 the average $g_{SS}(r)$ is sensitive to the sequence, as might be expected from the chain conformations. For f = 0.75 the first peak is more intense for Mg^{2+} counterions than Na^+ counterions, while the opposite is true for f = 0.25. This apparently counterintuitive result can be explained by considering conformations of chain for f = 0.25. For Na^+ counterions, the closest charged groups maintain their separation, while for Mg^{2+} counterions charged groups are more regularly distributed on the exterior, and this results in the first peak for Na^+ counterions being more intense than that for Mg^{2+} counterions.

The pair correlation functions between aromatic carbon atoms at the para position with respect to that connected to backbone ($g_{pCpC}(r)$) are insensitive to f or the nature of the counterions (see Figure 7). There are three main peaks at

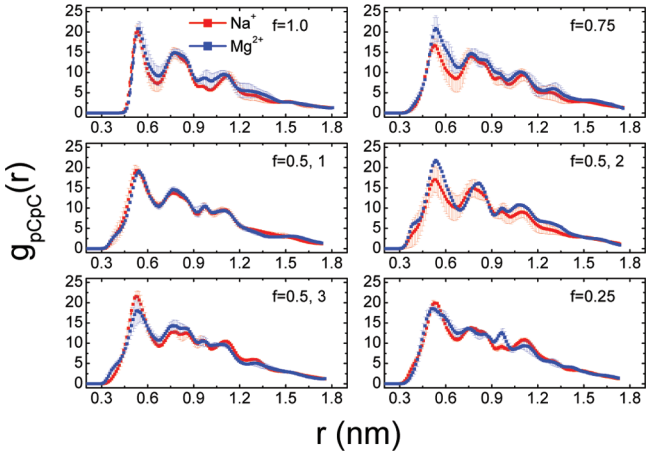

Figure 7. Pair correlation function between carbon atoms of side groups at para position with respect to that attached to the backbone for N = 16 and various values of f with Na^+ (red curves) and Mg^{2+} (blue curves) counterions. For f = 0.5 the different graphs correspond to different sequence isomers. The error bars are one standard deviation about the mean.

approximately r = 0.5, 0.8, and 1.1 nm, and a weaker peak at approximately r = 0.95 nm. The position and magnitude of these peaks is only weakly sensitive to the nature of counterions or value of f. This is surprising because the conformational properties are quite sensitive to these parameters. The insensitivity of $g_{pCpC}(r)$ may be because even when the chain is collapsed, this occurs through changes in only one dihedral angle, and therefore does not make a significant difference to the correlation between the benzene rings.

D. Counterion Distribution and Dynamics. The correlation between the Na^+ counterion and the sulfonate group is much stronger than that between the Mg^{2+} counterion and the sulfonate group (Note that initial configurations are prepared without contact ion pairs between the Mg^{2+} counterions and sulfonate groups.) Figure 8 depicts the counterion-sulfur correlation function for all cases studied. With the Na^+ counterions, $g_{NaS}(r)$ has a strong peak at r = 0.36 nm and a second peak at r = 0.56 nm. The first peak corresponds to the distance of closest approach of the counterion to the sulfonate group, and may be interpreted as a contact ion pair, while the second peak corresponds to a solvent separated ion pair, with a water molecule between the counterion and the sulfonate group. As f is increased from 0.25 to 1, the height of the first peak increases dramatically, by a factor of 3−4. This is because the electrostatic correlations are much stronger when the polymer is more strongly charged. The first peak is also higher for N = 16 than N = 8, as a consequence of the greater charge density near the longer chain.

With the Mg^{2+} counterions, the contact ion pair is absent in all cases. The first peak in $g_{MgS}(r)$ occurs at r = 0.53 nm and the second peak is at r = 0.73 nm. At first glance this is surprising because one expects a stronger correlation between a divalent ion and a sulfonate group. However, the correlation between

dx.doi.org/10.1021/jp208138t | J. Phys. Chem. B 2012, 116, 4319−4327

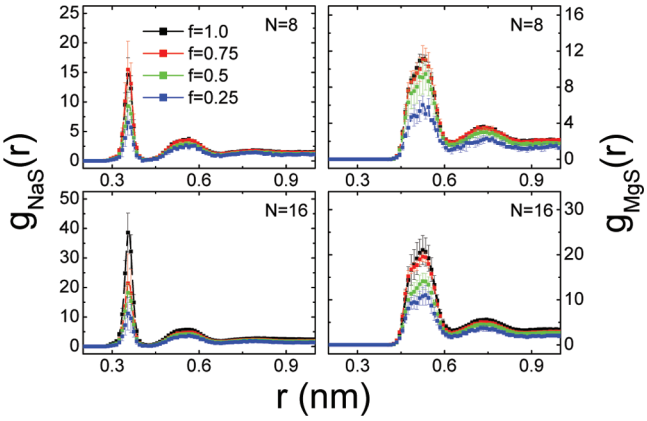

Figure 8. Pair correlation function between counterion and sulfur atom in the sulfonate groups. The error bars are one standard deviation about the mean.

Mg^{2+} and water is also stronger than that between Na^+ and water. Therefore the Mg^{2+} counterions are more strongly hydrated, and the first peak in $g_{MgS}(r)$ occurs at a distance corresponding to the closest approach between a hydrated Mg^{2+} ion and the sulfonate group; in fact this distance (0.53 nm) is quite similar to that of the solvent separated ion pair in the Na^+ case (second peak at 0.56 nm). The second peak in $g_{MgS}(r)$ corresponds to the correlation between a solvent separated hydrated Mg^{2+} ion and the sulfonate group. When either f or N increases, the height of the peak in $g_{MgS}(r)$ increases.

The stronger correlation between Na^+ (as opposed to Mg^{2+}) counterions and the sulfonate group can be explained using hydration effects. The interactions between SO_3^- group with multivalent counterions are thought to be stronger than those with monovalent counterions because of the higher charge on divalent counterions. However, divalent counterions also interact more strongly with water. This can be seen in the mean residence time of water molecules in the first solvation shell of counterions. We estimated the mean residence time for water in the vicinity of Na^+ counterions to be 25 ps, and that in the vicinity of Mg^{2+} counterions was greater than 75 ns. The long residence time of water molecules in the first solvation shell of Mg^{2+} ion is consistent with that given in ref 47. The interaction between Mg^{2+} and the sulfonated group are weakened by the fact that they are mediated by strongly bound water molecules, which restrict their mutual approach. Similar conclusions are obtained by comparing pair correlation function between counterions and water, where the peak positions in $g_{NaO}(r)$ and $g_{MgO}(r)$ are r = 0.23 and 0.2 nm, respectively, and the peak heights are 8 and 24, respectively (not shown).

An important concept in polyelectrolyte physics is that of counterion condensation or localization. In Manning's model,[48] counterions condense near the charged groups of polymer when the charge density along polyelectrolyte backbone is sufficiently high, i.e., $\xi = l_B/b > |z_i z_p|^{-1}$, where $l_B = e^2/(4\pi\varepsilon\varepsilon_0 k_B T)$ is the Bjerrum length, b is the average distance between charged groups, z_i and z_p are the valence of coutnerion and charged group of polymer, respectively. For PSS chains with f = 1, l_B = 0.715 nm and b = 0.285 nm, and counterion condensation is expected for $f > 0.4$ with Na^+ counterions and $f > 0.2$ with Mg^{2+} counterions. As can be seen in Figure 8 there is only a continuous change in the value of the pair correlation function as the charge fraction is increased, and the peak is weaker for Mg^{2+} than Na^+, contrary to the predictions of the Manning theory.

The counterions are also very mobile. In order to investigate the dynamics of counterions around PSS, we define a counterion-SO_3^- pair complex as being when the separation between the S atom and the counterion is smaller than a cut off distance r_c. The cut off distance corresponds to the position of the first minima in pair correlation function between counterion and sulfonate group (r = 0.43 and 0.63 nm for Na^+ and Mg^{2+}, respectively). We define the mean residence time (τ) of counterion around polymer as the lifetime of a counterion-SO_3^- group complex.

Figure 9 depicts τ as a function of f for all the cases studied. Contrary to expectations from localization, the lifetime of a

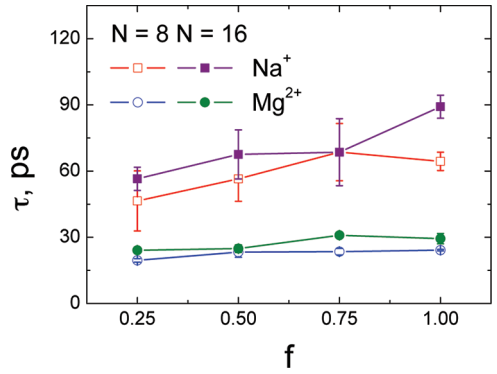

Figure 9. Residence time τ of counterions near sulfur atoms as a function of degree of sulfonation f. The error bars are one standard deviation about the mean.

counterion near the sulfonate group is extremely short, about 30−90 ps in all cases. For the same value of f and N, τ is higher for Na^+ than it is for Mg^{2+}. This is consistent with the Na^+ ions being more strongly correlated with the sulfonated groups than the Mg^{2+} ions. As f increases from 0.25 to 1, τ for Na^+ increases by about a factor of 3, as a consequence of the stronger electrostatic interaction. However, τ for Mg^{2+} does not depend on f and N, because of the screening of the electrostatic interactions by the tightly bound solvent molecules in the first solvation shell.

Similar conclusions are obtained by examining the fraction, $p(N_S)$, of counterions that are coordinated (within a distance of r_c) with N_S sulfonate groups (not shown). The majority of counterions are not coordinated with any SO_3^- groups even at the highest degree of sulfonation (f = 1), and only small fraction of counterions form a complex with charged groups, which increases with f and N.

E. Sampling Issues with Mg^{2+} Counterions. We find that MD simulations do not properly sample configurations of Mg^{2+} counterions because of the high free energy barrier to the formation and breaking of a contact pair between the sulfonate group and the Mg^{2+} counterion. In the results reported in the previous section, where initial configurations had no contact ion pairs, none were formed. We also simulated cases where the initial configuration has a contact pair between Mg^{2+} counterion and SO_3^- group(s), and these contact pairs persisted throughout the simulation, i.e., the contact pair has a lifetime greater than 75 ns.

The sulfonate Mg^{2+} contact ion pair is the thermodynamically stable state but there is a high barrier to formation. Figure

dx.doi.org/10.1021/jp208138t | J. Phys. Chem. B 2012, 116, 4319−4327

10 depicts the potential of mean force between a sulfur atom and Mg^{2+} counterion for a PSS dimer (f = 1) in water. The

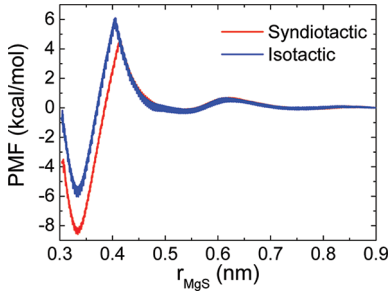

Figure 10. Potential of mean force (PMF) between the sulfur atom of a sulfonate group and a Mg^{2+} counterion for a PSS dimer with f = 1. The reaction coordinate, r_{MgS}, is the distance between the sulfur and Mg^{2+} particles. The error bars are one standard deviation about the mean.

potential of mean force (PMF) is calculated using a 10 ns umbrella sampling simulation with properties averaged over the last 9 ns. The reaction coordinate is the distance between these atoms (r_{MgS}). The barrier for the formation of the contact pair is approximately 4−6 kcal/mol (8−12 k_BT), depending on the tactility of the dimer, and that for the breaking of the contact pair is 12 kcal/mol (~24k_BT). Formation of a contact pair is therefore a rare event and once it is formed it is very stable, with an estimated lifetime of the order of 100 μs.

The stability of the contact ion pair is verified by simulations of 16-mer PSS chains (f = 1) with initial configurations in which all Mg^{2+} ions are paired with the sulfur atoms either in contact or separated by a water molecule. During an entire 100 ns simulation, the Mg^{2+} ion in the contact pair remains in the vicinity of its partner and no formation or breaking of the contact pair is observed. The Mg^{2+} ions in pairs separated by a water molecule, however, migrate along the PSS side groups as well as diffuse into the bulk water.

IV. SUMMARY AND CONCLUSIONS

We present results of atomistic simulations of polystyrene sulfonate in salt free aqueous solutions with Na^+ and Mg^{2+} counterions. Standard molecular dynamics simulations do not efficiently sample conformational space even during fairly long (100 ns) trajectories because of the restricted rotation of dihedral angles of backbone. The result is a trajectory to trajectory variation in the distribution of radius of gyration monitored in these simulations. We show that HREMD simulations better sample conformational space and this is the method of choice for these simulations. We also find that properties averaged over three independent MD trajectories (with different initial configurations) are similar to the HREMD results for the cases we study.

We observe a transition from collapsed to extended chain conformations as the sulfonation fraction (f) is increased. However, the compaction of the chain occurs through the (significant) change of only one or two dihedral angles. The collapse of these oligomers is therefore significantly different from the collapse of generic freely jointed chains of the same degree of polymerization. In the partially (or fully) collapsed configurations the charged groups are located on the outside and the benzene rings are buried, as might be expected. For f = 0.5 we investigate several sequence isomers which correspond to different groups being sulfonated. The conformations are sensitive to the placement of the sulfonated groups. Interestingly, for some cases the chains are more compact with Mg^{2+} counterions while in other cases the chains are more compact with Na^+ counterions.

The intrachain pair correlation functions are not very sensitive to the chain conformations. This can be explained by noting that the compaction occurs by the change of only a few dihedral angles and the average intrachain distances between atoms less than 1 nm apart therefore do not change much. This is even true for the sulfonate groups which are on the outside of the globules.

The molecular dynamics simulations do not sample configurations with Mg^{2+} counterions. The potential of mean force between a Mg^{2+} counterion and the sulfur atom on a PSS dimer has a high barrier (~8 −12 k_BT depending on the tactility) and a deep minimum (~−12 to −16 k_BT). The barrier is related to the dehydration of the Mg^{2+} counterion that is necessary before a contact ion pair can be formed. No forming or breaking of contact ion pairs (with Mg^{2+} counterions) is observed in any of the simulations. A proper sampling of counterion configurations should therefore employ advanced sampling (probably Monte Carlo) methods that specifically allow ion dehydration and contact pair formation. Of course, use of these methods will naturally preclude studying the dynamics of the Mg^{2+} counterions.

Another implication is in the use of implicit solvent methods of these systems. The Mg^{2+} counterions clearly exist in two states depending on the hydration level, and standard implicit solvent models ignore this feature.

For the case where the initial configurations do not contain contact pairs the Na^+ counterions are more strongly correlated with the sulfonate groups than the Mg^{2+} counterions. This is because the Mg^{2+} counterions are strongly hydrated and have to lose the hydration shell in order to approach the sulfonate groups closely. In all the cases, the counterion lifetime is quite short, of the order of 100 ps, and there is no counterion condensation. Consistent with the correlation functions, the Na^+ counterions have a longer lifetime at the sulfonate group than the Mg^{2+} counterions.

These results have some implications for generic bead−spring models of polyelectrolytes, where a group of monomers is replaced with a bead, and beads are connected by springs. Given the nature of the collapse of the 16-mer we conclude that a single "bead" must be composed of at least 16 chemical monomers. Since N = 40−700 in most experiments, this implies that most of these studies are not in the asymptotic large N limit, with less than 50 statistical segments. The simulations also emphasize the importance of solvent and counterion effects. For example, hydration effects cause the Na^+ counterions to be more strongly correlated with the sulfonate group than the Mg^{2+} counterions when the first hydration shell of the Mg^{2+} counterion is complete. However, merely using a larger diameter for the Mg^{2+} counterion is not appropriate because under some conditions the counterions shed the solvent molecules and condense onto the polymer. When the Mg^{2+} counterions form contact pairs with the sulfonate groups, these pairs are very stable so that the Mg^{2+} ions are much more strongly correlated with the sulfonate group than Na^+ ions. Because of such complexity, clearly some degree of chemical detail and incorporation of solvent might be key for an understanding of polyelectrolyte solutions.

dx.doi.org/10.1021/jp208138t | J. Phys. Chem. B 2012, 116, 4319−4327

Our simulations are restricted to fairly short chains because atomistic simulations for longer chains (in the experimentally interesting range) is prohibitively expensive at present. The fact that standard MD does not sample configurational space efficiently exacerbates this problem especially as the chain length is increased and there are more torsional degrees of freedom. Furthermore, most experiments are not for dilute solutions, and sampling issues might become more severe for semidilute and concentrated solutions.

A possible direction is the development of coarse-grained models for polyelectrolyte solutions where three or four heavy atoms are merged into a single coarse-grained site. This represents a compromise between detailed atomistic and generic models. This would be a good alternative for simulation studies of polyelectrolytes, which may bridge the gap between the complexity of the real systems and the simplicity of generic models. The development of such models for polymers, along the lines of what is done for peptides and lipids, is an important future direction of this work.

APPENDIX

Hamiltonian Replica Exchange Algorithm

In the HREMD simulations we scaled the Lennard-Jones (LJ) and electrostatic interactions between PSS atoms. The charges on the counterions were also scaled in order to maintain charge neutrality. A set of modified forcefields, denoted by the index k, is thus generated where a factor of $c_k \leq 1$ multiplies the charges of PSS atoms/counter ions and the strength of LJ potential between PSS atoms ($c_0 = 1$ and $c_k > c_{k+1}$). The potential energy term of Hamiltonian k (for the force-field k) can be written as

$$E_k(q) = V_0(q) + c_k V_1(q) + c_k^2 V_2(q) \quad (4.1)$$

where $q \equiv \{\mathbf{q}_1, ..., \mathbf{q}_{N_p}\}$ is the set of co-ordinates with N_p number of atoms in the system, V_0 unmodified term of potential energy, V_1 the sum of LJ PSS-PSS interactions and electrostatic interactions between PSS/conter ion and solvent atoms, and V_2 the electrostatic interactions between PSS/counter ion atoms.

We use 8 replicas in the HREMD simulations. The optimal scaling factors (tabulated in Table 2) are obtained from short

Table 2. Values of Scaling Factors for Hamiltonian Replica Exchange Molecular Dynamics Simulations

	c_k	
f	$N = 8$	$N = 16$
1	$1 - 0.024k$	$1 - 0.0165k$
0.75	$1 - 0.027k$	$1 - 0.0190k$
0.5	$1 - 0.031k$	$1 - 0.0225k$
0.25	$1 - 0.045k$	$1 - 0.0305k$

HREMD simulations. Exchange attempts are made every 5000 steps (10 ps) between neighboring replicas in an alternating sequences of exchange attempts for all even and odd pairs, e.g., pairs 0-1, 2-3, 4-5, and 6-7 at steps 5000, 15000, etc. and pairs 1-2, 3-4, and 5-6 at steps 10000, 20000, etc. Note that this exchange scheme is reasonable for the case that the exchange probabilities between neighboring replicas is sufficiently higher than those between distant ones. The exchange between replicas is accepted according to the Metropolis criterion. The average exchange probability of exchange between neighboring replicas is 0.2−0.3, which suggests our scheme is reasonable.

The initial 4-ns of each trajectory is omitted from analysis and energies are saved every 1000 steps (2 ps). Data produced during HREMD simulations are combined with the weighted histogram analysis method (WHAM).[49] Since the HREMD simulations are performed at fixed NPT, the WHAM equations are independent of E_0. The autocorrelation time of the potential energy is in the sub-picosecond range, and a period of 10 ps between exchange attempts is long enough to ensure quasi-independence of a replica-exchange step from the previous one.

AUTHOR INFORMATION

Corresponding Author

*E-mail: yethiraj@chem.wisc.edu.

Notes

The authors declare no competing financial interest.

ACKNOWLEDGMENTS

This research was supported in part by National Science Foundation through Grants CHE-0717569 and CHE-0840494. We thank Dr. Jejoong Yoo for implementation of CHARMM forcefield into GROMACS.

REFERENCES

(1) Dobrynin, A. V. *Curr. Opin. Colloid Interface Sci.* **2008**, *13*, 376.
(2) Volk, N.; Vollmer, D.; Schmidt, M.; Oppermann, W.; Huber, K. Polyelectrolytes with Defined Molecular Architecture II. *Adv. Polym. Sci.* **2004**, *166*, 29.
(3) Holm, C.; Joanny, J. F.; Kremer, K.; Netz, R. R.; Reineker, P.; Seidel, C.; Vilgis, T. A.; Winkler, R. G. Polyelectrolytes with Defined Molecular Architecture II. *Adv. Polym. Sci.* **2004**, *166*, 3.
(4) Grosberg, A. Y.; Nguyen, T. T.; Shklovskii, B. I. *Rev. Mod. Phys.* **2002**, *74*, 329.
(5) Barrat, J.-L.; Joanny, J. F. *Adv. Chem. Phys.* **1996**, *94*, 1.
(6) Forster, S.; Schmidt, M. Physcial Properties of Polymers. *Adv. Polym. Sci.* **1995**, *120*, 51.
(7) Spiteri, M. N.; Williams, C. E.; Boue, F. *Macromolecules* **2007**, *40*, 6679.
(8) Combet, J.; Isel, F.; Rawiso, M.; Boue, F. *Macromolecules* **2005**, *38*, 7456.
(9) Qu, D.; Baigl, D.; Williams, C. E.; Mohwald, H.; Fery, A. *Macromolecules* **2003**, *36*, 6878.
(10) Prabhu, V. M.; Muthukumar, M.; Wignall, G. D.; Melnichenko, Y. B. *J. Chem. Phys.* **2003**, *119*, 4085.
(11) Buhler, E.; Boue, F. *Eur. Phys. J. E* **2003**, *10*, 89.
(12) Dubois, E.; Boue, F. *Macromolecules* **2001**, *34*, 3684.
(13) Zhang, Y. B.; Douglas, J. F.; Ermi, B. D.; Amis, E. J. *J. Chem. Phys.* **2001**, *114*, 3299.
(14) Spiteri, M. N.; Boue, F.; Lapp, A.; Cotton, J. P. *Physica B* **1997**, *234*, 303.
(15) Spiteri, M. N.; Boue, F.; Lapp, A.; Cotton, J. P. *Phys. Rev. Lett.* **1996**, *77*, 5218.
(16) Baigl, D.; Sferrazza, M.; Williams, C. *Europhys. Lett.* **2003**, *62*, 110.
(17) deGennes, P. G.; Pincus, P.; Velasco, R. M.; Brochard, F. *J. Phys.-Paris* **1976**, *37*, 1461.
(18) Muthukumar, M. *J. Chem. Phys.* **1996**, *105*, 5183.
(19) Yethiraj, A. *Phys. Rev. Lett.* **1997**, *78*, 3789−3792.
(20) Yethiraj, A. *J. Chem. Phys.* **1998**, *108*, 1184.
(21) Shew, C. Y.; Yethiraj, A. *J. Chem. Phys.* **1999**, *110*, 5437.
(22) Shew, C. Y.; Yethiraj, A. *J. Chem. Phys.* **1999**, *110*, 11599.
(23) Shew, C. Y.; Yethiraj, A. *J. Chem. Phys.* **2002**, *116*, 5308.
(24) Yethiraj, A. *J. Phys. Chem. B* **2009**, *113*, 1539.
(25) Stevens, M. J.; Kremer, K. *J. Chem. Phys.* **1995**, *103*, 1669.
(26) Stevens, M. J.; Kremer, K. *J. Phys. II* **1996**, *6*, 1607.

(27) Winkler, R. G.; Gold, M.; Reineker, P. *Phys. Rev. Lett.* **1998**, *80*, 3731.
(28) Chang, R. W.; Yethiraj, A. *J. Chem. Phys.* **2002**, *116*, 5284.
(29) Chang, R. W.; Yethiraj, A. *J. Chem. Phys.* **2003**, *118*, 11315.
(30) Chang, R. W.; Yethiraj, A. *Macromolecules* **2005**, *38*, 607.
(31) Liu, S.; Muthukumar, M. *J. Chem. Phys.* **2002**, *116*, 9975.
(32) Liu, S.; Ghosh, K.; Muthukumar, M. *J. Chem. Phys.* **2003**, *119*, 1813.
(33) Chang, R.; Yethiraj, A. *Macromolecules* **2006**, *39*, 821.
(34) Reddy, G.; Yethiraj, A. *Macromolecules* **2006**, *39*, 8536.
(35) Reddy, G.; Yethiraj, A. *J. Chem. Phys.* **2010**, *132*, 74903.
(36) Chang, R. W.; Yethiraj, A. *J. Chem. Phys.* **2001**, *114*, 7688.
(37) Chang, R. W.; Yethiraj, A. *J. Chem. Phys.* **2003**, *118*, 6634.
(38) Reith, D.; Meyer, H.; Muller-Plathe, F. *Macromolecules* **2001**, *34*, 2335.
(39) Reith, D.; Muller, B.; Muller-Plathe, F.; Wiegand, S. *J. Chem. Phys.* **2002**, *116*, 9100.
(40) Molnar, F.; Rieger, J. *Langmuir* **2005**, *21*, 786.
(41) Chialvo, A. A.; Simonson, J. M. *J. Phys. Chem. B* **2005**, *109*, 23031.
(42) Laguecir, A.; Ulrich, S.; Labille, J.; Fatin-Rouge, N.; Stoll, S.; Buffle, J. *Eur. Polym. J.* **2006**, *42*, 1135.
(43) Carrillo, J.-M. Y.; Dobrynin, A. V. *J. Phys. Chem. B* **2010**, *114*, 9391.
(44) Hess, B.; Kutzner, C.; van der Spoel, D.; Lindahl, E. *J. Chem. Theory Comput.* **2008**, *4*, 435.
(45) MacKerell, A.; Bashford, D.; Bellott, M.; Dunbrack, R.; Evanseck, J.; Field, M.; Fischer, S.; Gao, J.; Guo, H.; Ha, S.; Joseph-McCarthy, D.; Kuchnir, L.; Kuczera, K.; Lau, F.; Mattos, C.; Michnick, S.; Ngo, T.; Nguyen, D.; Prodhom, B.; Reiher, W.; Roux, B.; Schlenkrich, M.; Smith, J.; Stote, R.; Straub, J.; Watanabe, M.; Wiorkiewicz-Kuczera, J.; Yin, D.; Karplus, M. *J. Phys. Chem. B* **1998**, *102*, 3586.
(46) Bjelkmar, P.; Larsson, P.; Cuendet, M. A.; Hess, B.; Lindahl, E. *J. Chem. Theory Comput.* **2010**, *6*, 459.
(47) Callahan, K. M.; Casillas-Ituarte, N. N.; Roeselova′, M.; Allen, H. C.; Tobias, D. J. *J. Phys. Chem. A* **2010**, *114*, 5141.
(48) Manning, G. S. *J. Chem. Phys.* **1969**, *51*, 924.
(49) Kumar, S.; Bouzida, D.; Swendsen, R. H.; Kollman, P. A.; Rosenberg, J. M. *J. Comput. Chem.* **1992**, *13*, 1011.